

Philippe Jodin¹, Hama Zedira², Zitouni Azari¹, Joseph Gilgert¹

FATIGUE LIFE ASSESSMENT OF AN EXCAVATOR ARM BOX Experiments and Computations

OCENA ZAMORNOG VEKA KUTIJE RUKE BAGERA Eksperimenti i proračuni

Originalni naučni rad / Original scientific paper
UDK /UDC: 620.169.1:621.879
Rad primljen / Paper received: 19.01.2009.

Adresa autora / Author's address:

¹) Laboratoire de Fiabilité Mécanique-Université Paul Verlaine-Metz et École Nationale d'Ingénieurs de Metz, France
jodin@univ-metz.fr

²) Département de Génie Mécanique – Centre Universitaire Larbi Ben M'Hidi, Algeria

Keywords

- weld
- structure
- fatigue
- fracture
- volumetric methods

Abstract

Arms of excavators are often made from box-beams, welded of steel plates. This work considers the problem of fatigue and fracture of welded parts of the excavator arm. Necessary data for fatigue tests of arm box beams include chemical composition, microstructure of steel and welds, as well as their mechanical properties and fatigue behaviour.

For results analysis Neuber's approach is used. Stress distribution is computed by a finite element method, and results are used to determine analytically effective distance and effective stress. Then k_f factor has been determined and the corresponding effective stresses derived.

Results have shown that experimental data and predictions fit quite well, but the number of experiments is still low to allow for any definitive conclusion. In any case, it has been shown by applied method that life duration of arm box-beams can be predicted with satisfying accuracy.

INTRODUCTION

The industry for mechanical production of structures is recently developed in Algeria, including the construction of excavators for civil engineering. The structure of excavator arm is designed as box and produced by welding. In service it is exposed to variable loads. The stress concentration at imperfections and defects induced by welding is responsible for fatigue crack initiation and growth up to final fatigue fracture. This paper is focused on the fatigue resistance evaluation of welded arm structure and the method for its service life prediction. Service experience shows that cracks from weld root extended to the shoe of box, where bend stress is the highest, and ends in fracture (Fig. 1).

Ključne reči

- zavar
- struktura
- zamor
- lom
- zapreminska metoda

Izvod

Ruka bagera se često izrađuje od kutijastih greda, zavarenih od čeličnih ploča. U ovom radu je razmatran problem zamora i loma zavarenih delova ruke bagera. Potrebni podaci za zamorna ispitivanja kutijaste grede ruke uključuju hemijski sastav, mikrostrukturu čelika i zavara, kao i njihove mehaničke osobine i zamorno ponašanje.

Za analizu rezultata je primenjen Nojberov pristup. Raspodela napona je sračunata metodom konačnih elemenata, a rezultati su korišćeni za analitičko određivanje efektivnog rastojanja i efektivnog napona. Zatim je određen faktor k_f i izvedeni su odgovarajući efektivni naponi.

Rezultati su pokazali da je saglasnost eksperimentalnih podataka i predviđanja veka dobra, ali je ipak broj eksperimenata još mali za konačne zaključke. U svakom slučaju je primenjenom metodom pokazano da se može predvideti radni vek kutijaste grede ruke sa dovoljnom tačnošću.

In order to get more insight in fatigue crack significance for excavator welded arm integrity and predict service life duration, extended experimental and numerical analysis has been performed.

EXPERIMENTAL ANALYSIS

Details of the experimental investigation are given in /1/.
Materials chemical composition and properties

Chemical compositions of base metal, Q36 steel, and weld metal SG-3, are given in Table 1, and mechanical properties in Table 2, according to German specifications.

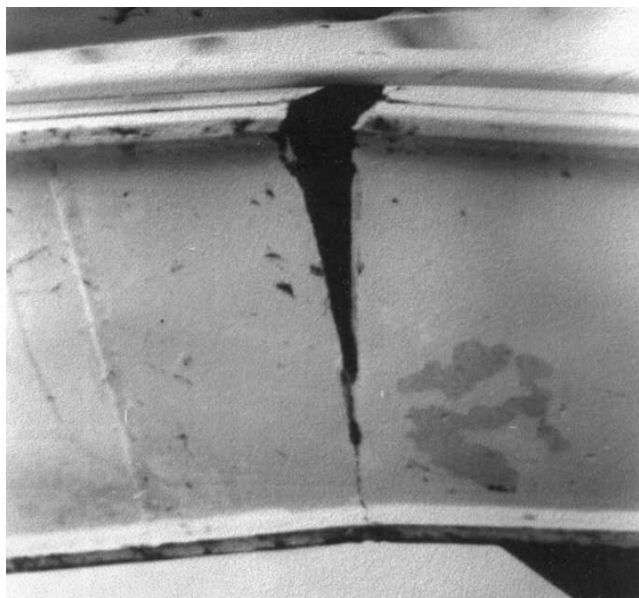


Figure 1. Final fracture of welded box.
Slika 1. Konačni lom zavarene kutije

Table 1. Specified chemical composition of base and weld metals.
Tabela 1. Propisan hemijski sastav osnovnog metala i metala šava

Material		C	Si	Mn	P	S	Ti
Base metal	Q36	0.16	0.50	1.60	0.03	0.03	0.12
Weld metal	SG-3	0.07–0.14	0.8–1.2	1.6–1.9	–	–	–

Table 1. Mechanical properties of base and weld metals.

Tabela 2. Mehaničke osobine osnovnog metala i metala šava

		Yield stress	Tensile strength	Impact energy	Elongation
Material		R_{e0} , MPa	R_m , MPa	KCV, J	%
Base metal	Q36	355	490–690	27	25
Weld metal	SG-3	470	590		30

Metallography

Metallographic analysis revealed the base metal of ferrite-pearlite microstructure (Fig. 2), weld metal of bainite microstructure (Fig. 3), and the heat-affected-zone (HAZ) in critical region close to the fusion line of typical bainite microstructure (Fig. 4) of the acceptable quality.

Fatigue tensile tests

The heterogeneity of welded joint microstructure (Figs. 2–4) affects its resistance to cracking. As the fatigue cracks in welded box frequently occurred in the weld root region, as presented in Fig. 1, fatigue properties of the base metal, welded joint and of welded box beam were necessary for numerical calculation and life prediction modelling. For that, fatigue tensile tests have been performed with smooth specimens of base metal and of welded joints, with weld overfill flash grinded to obtain a smooth surface and to reduce stress concentration (Fig. 5).

All tests were performed on a servohydraulic Instron testing machine, at frequency of 6 Hz. Selected load ratio R was $R = \frac{F_{min}}{F_{max}} = 0.1$, with minimum load F_{min} , and maximum load F_{max} in one cycle.

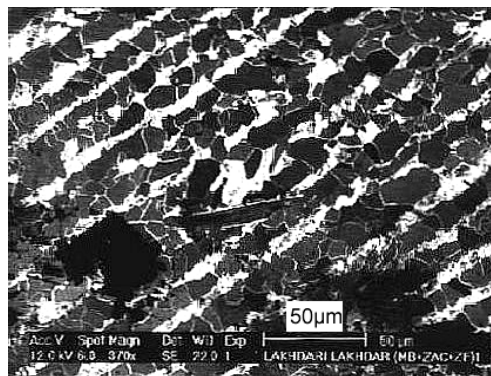


Figure 2. Ferrite pearlite microstructure of base metal.
Slika 2. Feritno-perlitna mikrostruktura osnovnog metala

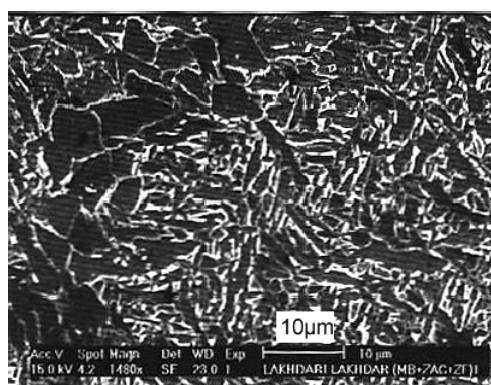


Figure 3. Microstructure of bainite dendrites in weld metal.
Slika 3. Mikrostruktura beinitnih dendrita u metalu šava

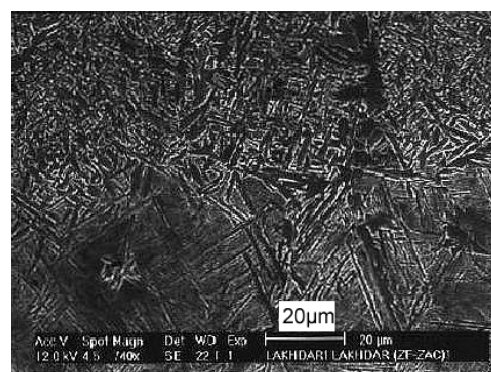


Figure 4. Heat-affected-zone close to the fusion line – bainite microstructure.

Slika 4. Zona uticaja toplote blizu linije stapanja – beinitna mikrostruktura

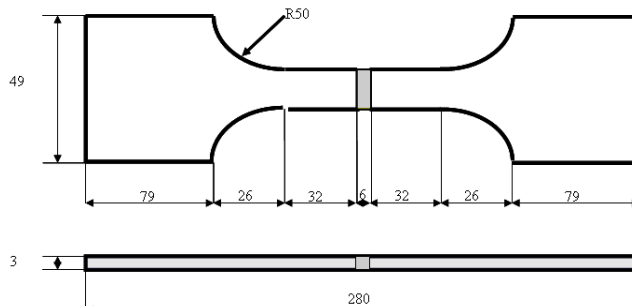


Figure 5. Smooth specimen for tensile fatigue test.
Slika 5. Glatka epruveta za ispitivanje zamora zatezanjem

Fatigue bending tests

In order to get closer insight into the fatigue behaviour of the excavator welded arm, special welded specimens for fatigue tests by three points bending were prepared, simulating arc box beam design (Fig. 6). Specimens, welded of Q36 steel plates, were prepared by following the specified technology for fabrication. To prevent excessive compressive

deformation in load contact point, a reinforcing plate is also welded in the middle of box upper side. The box model specimen was loaded by a three-point bending device, adapted to the servo-hydraulic testing machine (Fig. 7). The same frequency and *R* ratio as in fatigue tensile tests were applied also in the fatigue bending test.

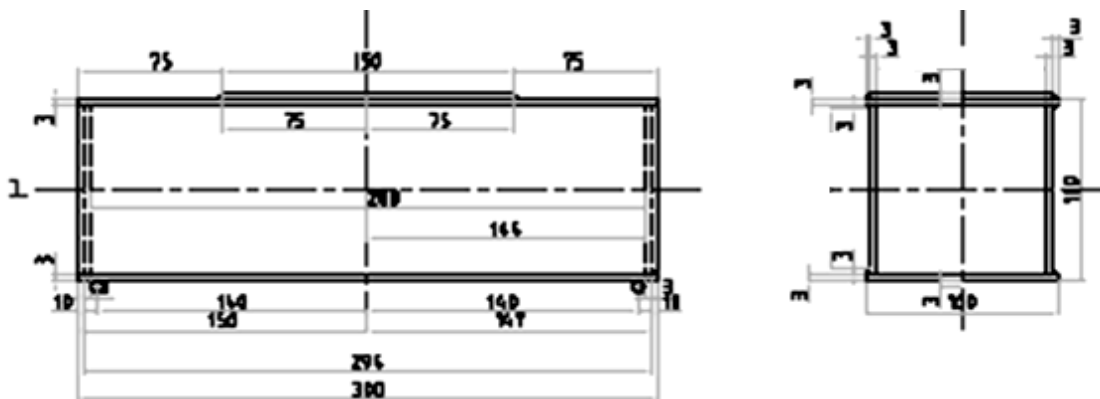


Figure 6. Bending fatigue test specimen produced as the model of excavator arm welded box.
Slika 6. Epruveta za ispitivanje zamora savijanjem izvedena kao model zavarene kutije ruke bagera

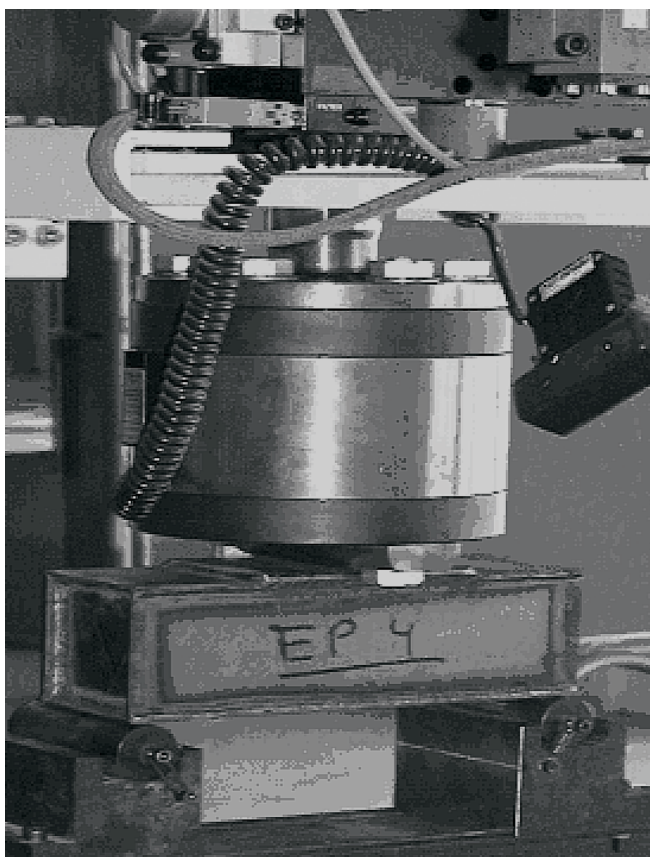


Figure 7. The arrangement of fatigue experiment by bending of box model specimen on testing machine.
Slika 7. Eksperimentalna postavka ispitivanja na zamor savijanjem epruvete modela kutije na kidalici

Results of fatigue tests

Results are given in terms of *S-N* curves (amplitude of stress, *S*, vs. number of cycles to fracture, *N*). Computa-

tional results were used for the analysis by the Neuber's approach, /2/, to determine the fatigue stress concentration factor, *k_f*, as a data necessary to predict the life duration of welded box beams, /3, 4/. Factor *k_f* is defined as the ratio of the stress amplitude for a smooth specimen and the stress amplitude for a notched specimen for a given number of cycles to fracture. In the experiments performed here, as smooth specimens the welded grinded tensile specimens are accepted (Fig. 5), and as notched ones the welded beam-box model specimens (Fig. 6).

Only five beam-box model specimens were available, provided by an Algerian company producing excavators. Despite of small number of specimens for that kind of test, the results seem to be reliable for life prediction modelling.

As an example, one fractured box beam specimen after testing is shown in Fig. 8. It can be clearly seen that a crack initiates at the bottom part of the specimen and propagates to the shoe of the beam, and then into the beam web. Pictures taken during fatigue tests allowed to indicate the precise location of crack initiation (Fig. 9).

The determination of crack initiation point at the root of the welded specimen allowed computing the applied normal bending stress, necessary for the definition of *S-N* curve of the boxes.



Figure 8. Fracture of box specimen in fatigue bending test.
Slika 8. Lom kutijaste epruvete u ispitivanju zamora savijanjem

NUMERICAL ANALYSIS

Finite element computations have been made to determine the amplitude of bending stress for each tested box specimen. The developed finite element mesh (Fig. 10) included also contact elements between different plates welded in the box (Fig. 11).



Figure 9. The High contrast in the image allowed to determine the precise location of fatigue crack initiation during testing.
Slika 9. Visok kontrast na slici omogućio je da se precizno odredi položaj inicijacije zamorne prsline pri ispitivanju

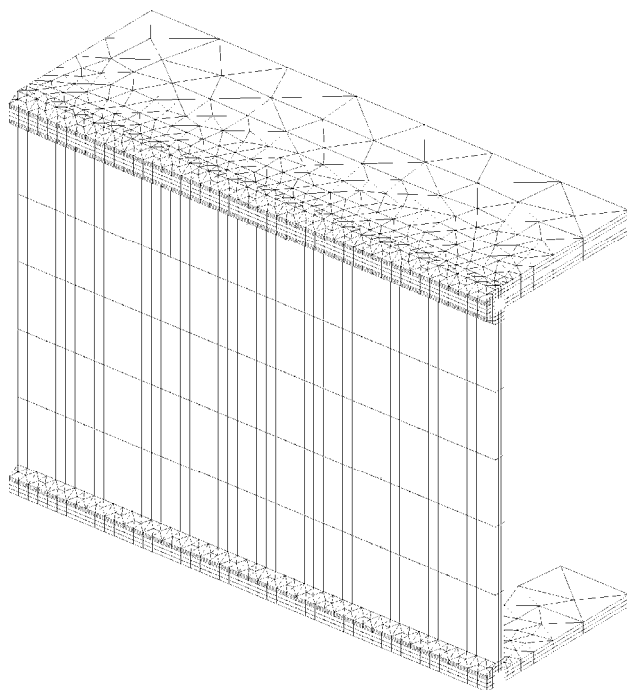


Figure 10. Finite elements mesh (one quarter of welded box).
Slika 10. Mreža konačnih elemenata (četvrtina zavarene kutije)

NUMERICAL ANALYSIS

Finite element computations have been made to determine the amplitude of bending stress for each tested box specimen. The developed finite element mesh (Fig. 10) included also contact elements between different plates welded in the box (Fig. 11).

The position for computing maximum normal bending stress amplitude is marked in Fig. 11, indicating also the location of fatigue crack initiation. In the performed computation the material is considered as elastic-plastic, and the applied load is taken as an uniformly distributed vertical force in the upper plate, in the plane of symmetry, where maximum bending stress is assumed to occur. Since the testing was performed with load ratio $R = 0.1$, the stress $\sigma(F_{max})$ was computed first for maximum load F_{max} , and then $\sigma(F_{min})$ for $F_{min} = F_{max}/10$. The stress amplitude $\Delta\sigma$ is calculated as

$$\Delta\sigma = \sigma(F_{max}) - \sigma(F_{max} / 10) \tag{1}$$

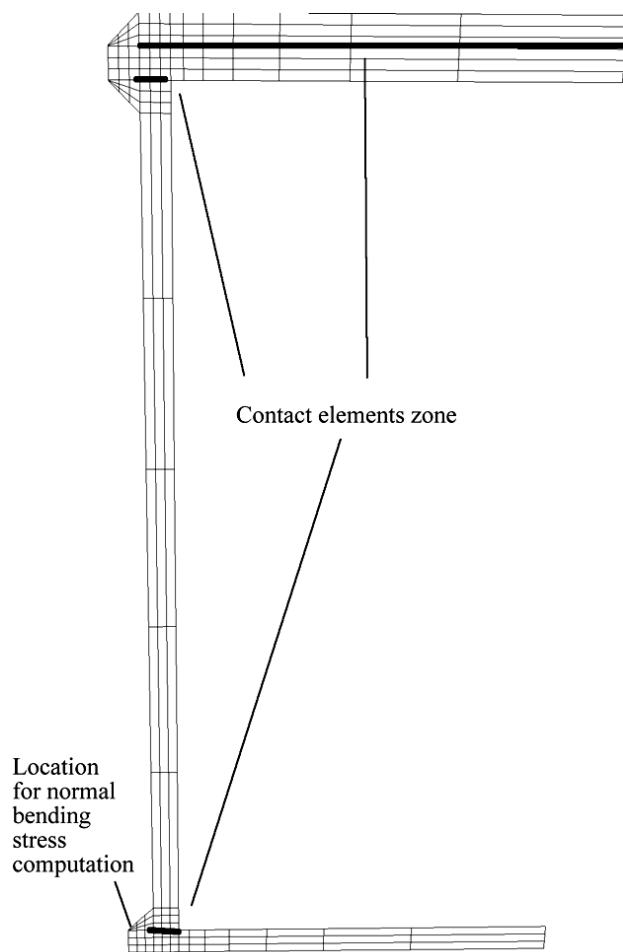


Figure 11. Marked contact element zones.
Slika 11. Označene zone kontaktnih elemenata

The stress amplitude $\Delta\sigma$ versus the number of cycles to fracture N_f is presented in Fig. 12 for:

- the reference smooth welded specimens (Fig. 5);
- here tested box specimens (Fig. 6); and
- the results of performed computations.

Experimental results are fitted according to Basquin’s law:

$$\Delta\sigma = A + B \cdot \ln(N_f) \tag{2}$$

with constants A and B taken from Ref. /1/.

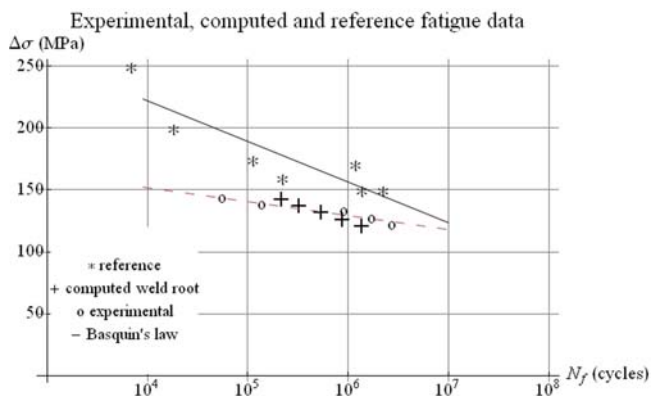


Figure 12. Experimental, reference and computed data.
Slika 12. Eksperimentalni, literaturni i sračunati podaci

Computation of stresses

The root of the weld, where the crack initiated, may be considered as a notch tip with a supposed radius. According to Panella, /5/, this radius could be taken as $\rho = 0.5$ mm.

Based on this value, the distribution according to Neuber, /6/, is assumed:

$$\sigma_{eff} = \sigma_{amx} \frac{1}{\sqrt{1 + \frac{4x_{eff}}{\rho}}} \tag{3}$$

In order to estimate the effective distance, x_{eff} , it is necessary to determine effective stress, σ_{eff} , for the application of Neuber's distribution. Pook et Frost, /7/, suggested the estimation:

$$x_{eff} = \frac{1}{\pi} \left(\frac{\Delta K_{th}}{\sigma_D} \right)^2 \tag{4}$$

where ΔK_{th} is the fatigue crack propagation threshold and σ_D is the fatigue limit. Following /7/, ΔK_{th} can be taken as:

$$\Delta K_{th} \cong 1.1 \cdot 10^{-5} \cdot E \tag{5}$$

where E is the Young's modulus.

It follows, based on the suggestion proposed by François, /8/, that σ_D can be taken as:

$$\sigma_D = \frac{R_m}{2} \approx 300 \text{ MPa} \tag{6}$$

Fatigue notch factor

Geometrical singularities, such as roots or notches, are the locations of stress concentration, and cracks preferably initiate in these regions. If a comparison between a smooth structure and a notched one is made, a fatigue notch factor can be defined as:

$$k_f = \frac{\Delta \sigma_s}{\Delta \sigma_n} \tag{7}$$

where $\Delta \sigma_s$ is the amplitude of stress producing the fracture at a given number of cycles for a smooth specimen, and $\Delta \sigma_n$ is the amplitude of stress producing the fracture for the same number of cycles for a notched specimen.

In the considered case, using experimental results, it was possible to derive a mean value of $k_f = 1.25$ for tested smooth specimens and box model specimens, /1/.

Life duration predictions

One of the goals in the computational part of this work was to predict the duration life in terms of number of cycles to fracture N_f of excavator arm beam boxes.

The applied approach was to compute by finite elements the bending stress at the location of crack initiation, then to derive the effective stress, using the Neuber's distribution. The next step was to determine fatigue notch factor k_f and finally, to derive the number of cycles to fracture. Results of performed computation are given in /1, 3, 4/. It can be underlined that the results of computation fit quite well with the experimental results.

DISCUSSION AND CONCLUSION

At first, it should be mentioned that the analysis is here based on only 5 experiments. Each experiment should be repeated several times to confirm the significance of results. In addition, as the box-beams specimens were not produced under our supervision, the quality of welding manufacture is questionable. Particularly, the exact location of crack initiation could not be determined. In post testing fractographic examination some unexpected defects had been found in fillet welded joints (Figs. 13, 14), indicating possible unexpected local stress concentration. However, these defects did not affect the results of the performed investigation, since fatigue cracks initiated in all specimens in locations of expected fatigue fracture.

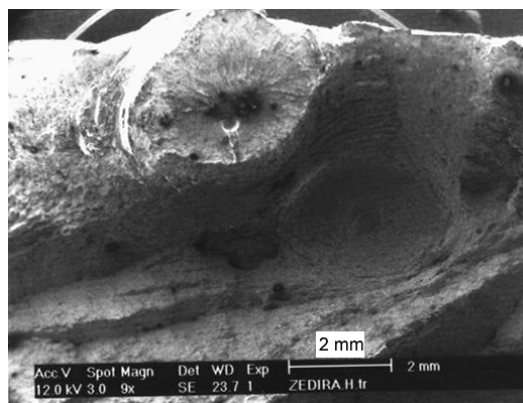


Figure 13. Typical "fish-eye" defect of welded joint.
Slika 13. Tipična greška "riblje oči" zavarenog spoja

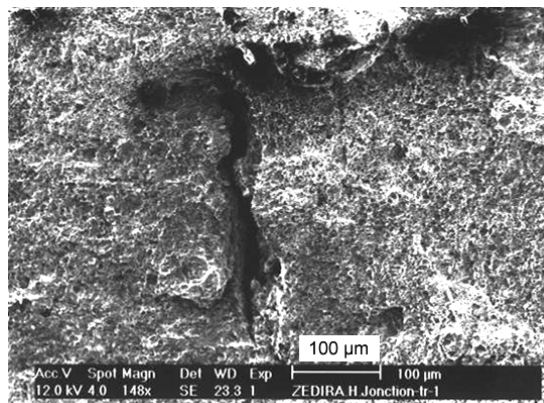


Figure 14. Transverse crack on fatigue fracture surface.
Slika 14. Poprečna prslina na površini zamornog preloma

Presented results have shown that the applied approach is suitable for life duration prediction, despite of minimum performed tests. This is confirmed by comparing the results obtained here with results of previous similar investigation, performed by Zedira et al., /4/, presented in Fig. 15.

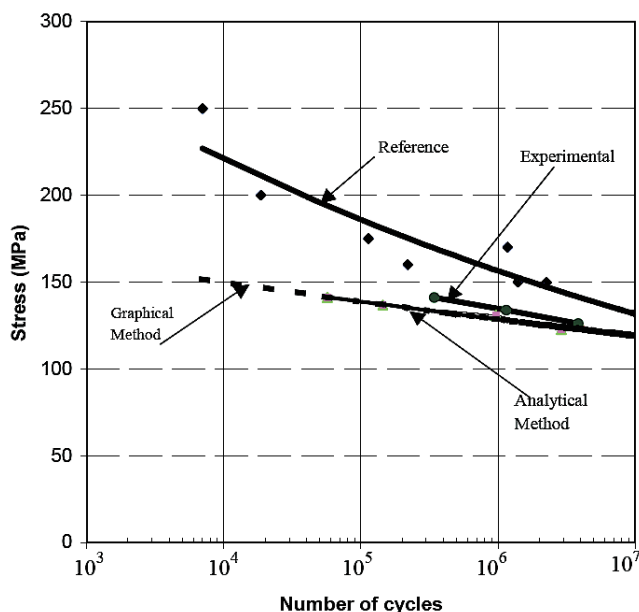


Figure 15. The results published in Ref. /4/.
Slika 15. Rezultati objavljeni u Ref. /4/

It should be noticed that only three experimental results were available when Ref. /4/ was published. The results of “analytical method” and “graphical method” in Fig. 15 are very similar. This is not surprising as they are both based on the volumetric approach. Otherwise, the authors in Ref. /4/ reported a k_f factor of 1.33, which is very close to the same factor in this paper ($k_f = 1.25$), so it is expected that the results should also be compatible.

However, in Ref. /4/ exact information about the location of crack initiation and computation processed are not given, as this is the case with the data about notch radius size used in computation, this comparison is in some aspects questionable. The agreement of all considered results is so good, that they can be accepted as successful and applicable.

The results presented here allow to conclude that the proposed approach and applied methods are quite accurate and usable for life duration prediction, in the considered case of beam-box arm of an excavator, because the range of predicted life is sufficiently close to the range obtained experimentally. However, it is possible that the prediction may be too pessimistic for high stress amplitudes and too optimistic for lower stress amplitudes, which should be examined in the next investigation.

REFERENCES

1. Zedira, H., *Etude mécanique, métallurgique et fissuration par fatigue des caissons soudés entrant dans la réalisation des engins de travaux publics*. PhD Thesis, Université El Hadj Lakhdar, Batna, Algeria (2005).
2. Neuber, H., *Theory of stress concentration for shear-strained prismatic bodies with arbitrary non-linear stress-strain law*, J. Appl. Mech., 28 (1961), 254.
3. Qylafku, G., Azari, Z., Kadi, N., Gjonaj, M., Pluvinage, G., *Application of a new model proposal for fatigue life prediction on V notches and keys-seats*, Int. J. Fatigue, 21 (1999), 753-760.
4. Zedira, H., Gilgert, J., Boumaza, A., Jodin, P., Azari, Z., Pluvinage, G., *Fatigue life prediction of welded box structures*, Strength of Materials, Vol. 36, No. 6 (2004), 558-564.
5. Panella, F.W., *Méthodes modernes pour le dimensionnement en fatigue de structures soudées*. PhD Thesis, Université de Metz & Università di Lecce, Metz, France (2000).
6. Shin, C.S., *Fatigue crack growth from stress concentrations and fatigue life predictions in notched components*. In: Handbook of Fatigue Crack Propagation in Metallic Structures, A. Carpinteri Ed., Elsevier Sciences B.V. (1994).
7. Pook, L.P., Frost, N.E., *A fatigue crack growth theory*, Int. J. Fatigue, 9 (1976), 53-61.
8. François, D., *Endommagements et rupture des matériaux*. INC NetLibrary, EDP Sciences Editions (2004).